Available online at www.sciencedirect.com
ScienceDirect
Journal of Power Sources 175 (2008) 547–552
JOURNAL OF POWER SOURCES
www.elsevier.com/locate/jpowsour

Short communication

The study of Mg_2Si/carbon composites as anode materials for lithium ion batteries

J.M. Yan [a,b], H.Z. Huang [a], J. Zhang [a], Y. Yang [a,*]

[a] *State Key Lab for Physical Chemistry of Solid Surface, Department of Chemistry, Xiamen University, Xiamen 361005, China*
[b] *Environment Science research Center, Xiamen University, Xiamen 361005, China*

Received 24 April 2007; accepted 14 June 2007
Available online 23 June 2007

Abstract

The study of Mg_2Si/C composites as anode materials for lithium ion batteries is reported in this paper. Firstly, Mg_2Si was synthesized by mechanically activated annealing (MAA) technique and the preparing conditions for pure Mg_2Si alloy were investigated and optimized. Then the composite materials of Mg_2Si and carbon materials such as CNTs and CMS with different ratios were prepared by the followed ball-milling techniques. Their electrochemical performances were compared by the galvanostatically charge/discharge and EIS experiments. The pure Mg_2Si alloy delivers a large initial capacity, but the capacity decreases rapidly with cycling. In contrast, the composites show good cyclic stability and deliver a reversible capacity of about 400 mAh g^{-1} with 40% carbon in the composite. The results of EIS indicate that the composite of Mg_2Si/CMS has better interface stability than that of pure Mg_2Si materials.

Keywords: Mg_2Si; Carbon; Composites; Anode material; Lithium ion batteries

1. Introduction

Lithium ion batteries are state-of-the-art power sources for portable electronic devices and electric vehicles. They have several advantages such as high energy density, long cycle life and no memory effect. In order to make high energy density battery (i.e. the specific energy density of the batteries is >200 Wh kg^{-1}), high capacity anode materials such as alloy compounds [1,2], transitional metal oxides [3–6] and lithium metal nitride [7,8] were explored in the recent years. Intermetallic alloy compounds were firstly proposed as Li storage materials by Anani and Huggins in 1992 [9]. Intermetallic electrode materials have shown some promises as anode materials for lithium batteries because of their ability to offer larger capacities than the graphite and better cycling performance than binary alloy [10–15].

Magnesium silicide (Mg_2Si) has several characteristics which make it an attractive candidate for lithium storage. First, lithium can be inserted electrochemically into magnesium, silicon and their alloy at room temperature [16,17], respectively. Second, both elements are naturally abundant and inexpensive. Third, large specific capacities may be achievable because both elements are light-weight.

Kim et al. [17] proposed a three-step mechanism based on lithium intercalation into Mg_2Si, after lithium intercalation limit was reached, the Mg_2Si structure was destroyed, forming binary Li–Mg and Li–Si alloys. Moriga et al. [18] reported a two-step mechanism, i.e. the formation of a unique ternary phase firstly, Li_2MgSi, and then forming Li–Si and Li–Mg alloys, respectively. Both of mechanisms undergo an alloying process, which leading to a poor cyclic performance due to high volume** expansion. Roberts et al. [19] synthesized Mg_2Si by mechanically activated annealing (MAA) method and studied its electrochemical performance and the lithiated mechanism. As it is expected, the cyclic stability of the Mg_2Si materials is poor.

The disadvantage of the Mg_2Si was that the alloying process with Li^+ does not appear to be sufficiently reversible due to large volume changes during cycling. Since some carbon materials especially hard-carbon materials can provide porous structure and tolerate some volume change of the materials during Li^+ intercalation/de-intercalation process, thus the silicide/carbon

* Corresponding author.
E-mail address: yyang@xmu.edu.cn (Y. Yang).

0378-7753/$ – see front matter © 2007 Published by Elsevier B.V.
doi:10.1016/j.jpowsour.2007.06.074

composites could be one of good choice for preventing the pulverization of alloy powders and improving its cyclic stability. The composites as anode materials for lithium ion batteries have been studied by several groups recently [20–31]. For example, Lee et al. [30] reported the graphite–FeSi alloy composites as anode materials for rechargeable lithium batteries and demonstrated the materials have quite a high reversible capacity with excellent cycleability. However, to the best of our knowledge, there are not reports about synthesis and the electrochemical performances of Mg_2Si/C composite materials in the literature.

In this work, we have synthesized pure Mg_2Si by MAA method and prepared Mg_2Si/C with different ratios of carbon nanotubes (CNTs) or carbonaceous mesophase spheres (CMS) by ball-milling method. The electrochemical performances of the samples were studied by the galvanostatically charge and discharge experiments and the ac impedance technique. The results indicate that the composite improves the electrochemical performances of Mg_2Si and the composite materials show a quite high reversible capacity and good cyclic stability.

2. Experimental

A planetary ball mill (Fritsch P-6 Planetary Mono Mill, Germany) was used to synthesize Mg_2Si from elemental powders. Mg (99.0%, Shanghai Xingzhi Chemical plant, China) and Si (99.9%, 300mesh, Taixinlong Co, Beijing, China) powder were added into a 80-ml carnelian grinding bowl with 10 carnelian balls of 10 and 5 mm and 3 ml hexane in an argon-filled glove box. Milling was performed at a rotation rate of 500 rpm for 5 h under inert gas atmosphere. The mixture was pressed into a plate at 30 MPa then annealed at 600 °C for 2 h in an argon atmosphere. After finishing preparation of Mg_2Si, The as-prepared Mg_2Si and CNTs, CMS in different weight proportions were, respectively, mixed and then milled at a rotation rate of 500 rpm for 3 h. The carbonaceous mesophase spheres (CMS) is bought from Shanshan Tech. Corp. (Shanghai, China) and the carbon nanotubes (CNTs) is provided by Prof. Zhang Hongbin's group as a gift [32]. The phases of the synthesized products were analyzed by an X-ray diffractometer (Panalytical X′Pert diffractometer with radiation operated at 40 kV and 30 mA, The Netherland). Data were collected in the range 10–90°.

The specific capacity and cyclic stability of the electrode materials were evaluated by using of in CR2025 coin cells,

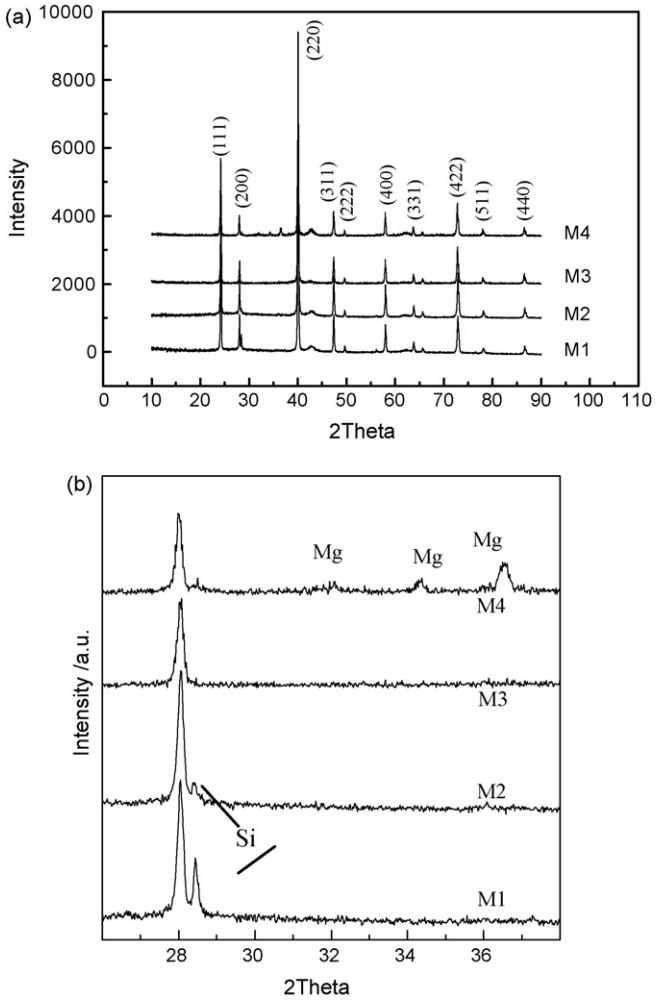

Fig. 1. The XRD patterns of Mg_2Si synthesized with different ratio of Mg and Si (a) 10–90°; (b) 24–40°. Here, M1, M2, M3 and M4 represent that the ratio of Mg and Si are 2.1:1, 2.18:1, 2.2:1 and 2.4:1, respectively.

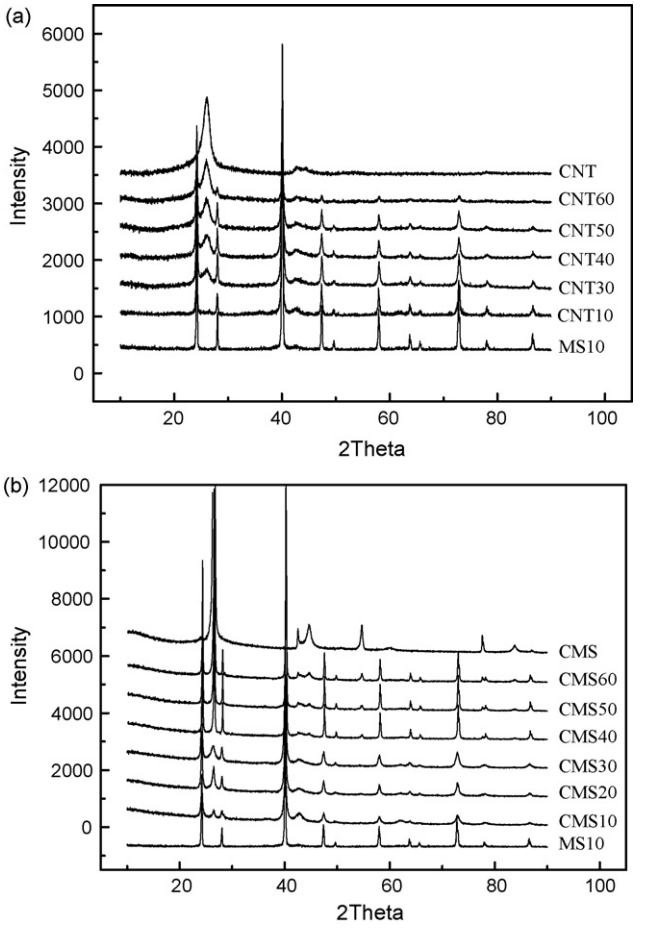

Fig. 2. XRD patterns for composites of Mg_2Si and carbon materials. (a) CNTs system; (b) CMS system.

which has been reported in our previous work [33,34]. The anode was prepared by mixing 75% of the active material with 15% carbon black and 10% poly(vinylidene fluoride) (PVDF). The mixture was made into slurry by ball-milling 3 h at a rotation rate of 500 rpm using *N*-methyl-2-pyrrolidene (NMP) (the water content was less than 0.01 wt.%) as the solvent. The working electrodes were formed by coating the slurry onto Cu foils and pressing at 20 MPa after drying overnight at 60 °C in a vacuum. The cells were assembled with the working electrode as prepared, with lithium metal as counter electrode, and with Celgard 2400 film as a separator. The electrolytes were 1 M $LiPF_6$ dissolved in EC + DMC (1:1 volume ratio). Cell assembly was carried out in an argon-filled glove box (LabMaster 100, MBraun, Germany), where water and oxygen concentrations were kept less than 3 ppm. Charge–discharge tests were performed galvanostatically at 50 mA g^{-1} current density between 0.02 and 3.0 V by a home-made LAND CT2001A battery tester. The EIS testing was carried out with a Solartron Instrument (1287 + 1260 electrochemical working station, Scribner Associates Inc. UK) by a three electrodes system and Li metal was used as the count and the reference electrode, respectively. The ac perturbation signal was ±10 mV and the frequency range was from 10 mHz to 3.2×10^7 Hz.

3. Results and discussion

3.1. XRD characterization of the materials

The XRD patterns of Mg_2Si synthesized are shown in Fig. 1. When the proportion of Mg and Si in the mixture was 2.1:1 (i.e. Mg: Si = 2.1:1, curve M1) to make the composites, a distinct Si peak appears in the products at 28.4°, but no pure Mg diffraction peak is observed. When the reactant proportion is increased to 2.18:1(curve M2), the intensity of Si peak decreased but still is observed. The ratio of Mg and Si is continually increased to 2.2:1 (curve M3), the pure Mg_2Si diffraction peaks are observed, but Si peak entirely disappeared and no Mg peak can be observed in the XRD patterns. However, when the stoichiometric ratio of Mg and Si reaches 2.4:1 (curve M4), the additional Mg peaks are detected. Thus, the best ratio of Mg and Si for preparation of pure Mg_2Si is 2.2:1, i.e. additional 10% of Mg should be added besides the normal ration of Si and Mg during the preparation process in order to get pure Mg_2Si. Based on the analysis of XRD pattern, the pure Mg_2Si has cubic structure with a space group F_{m3m} (JPCD 01-075-0445).

The XRD patterns for composite materials of Mg_2Si/CNT and Mg_2Si/CMS in different carbon ratio are shown in Fig. 2. Here, CNT10, CNT20, CNT30, CNT40, CNT50 and CNT60

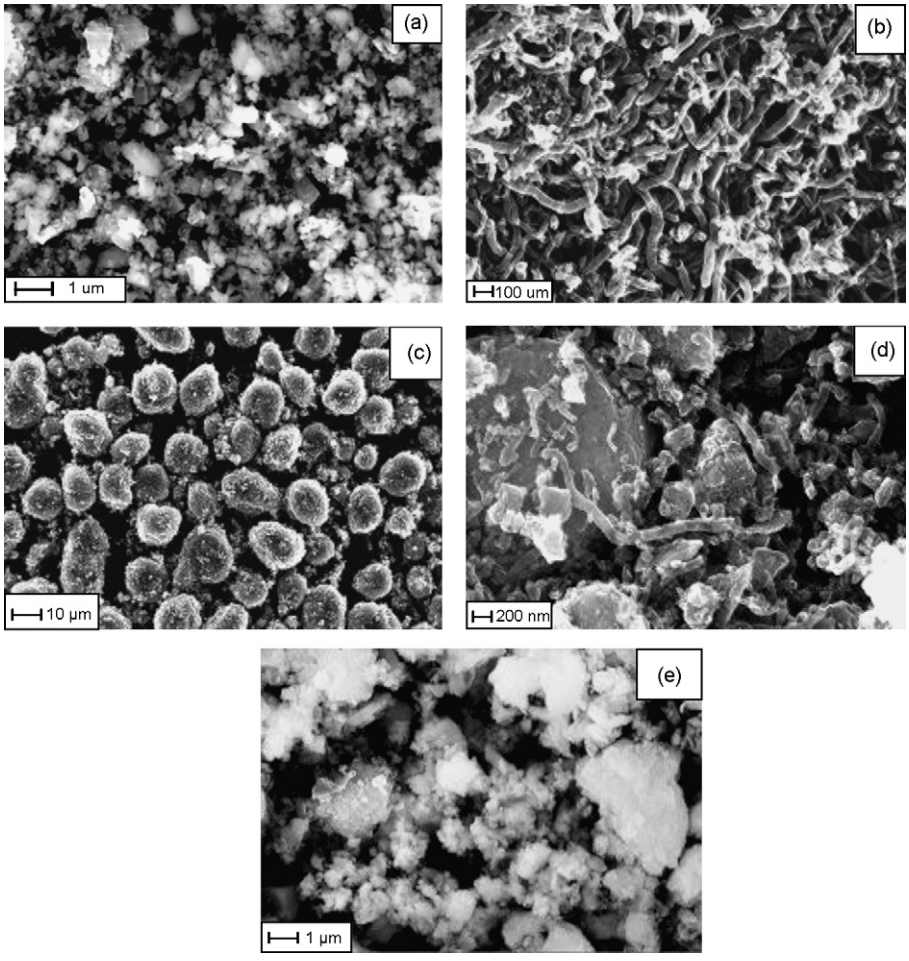

Fig. 3. The SEM images Mg_2Si (a), CNTs (b), CMS (c) and composites materials CNT40 (d) and CMS40 (e).

represent that the contents of CNTs in the composites are 10, 20, 30, 40, 50 and 60 wt.%, respectively. Similar representation is also used for Mg_2Si/CMS composite system. From Fig. 2, it is shown that the intensity of the peaks of CNTs and CMS increased with the carbon content, whereas the intensity of Mg_2Si peaks almost has not change. Otherwise, no new phase was observed in all composites based on XRD patterns.

3.2. SEM characterization

The SEM images Mg_2Si (a), CNTs (b), CMS (c) and composites materials CNT40 (d) and CMS40 (e) are shown in Fig. 3. Fig. 3a and b and c show that most of the Mg_2Si and CMS particle shape are spherical and the estimated average particle size of the Mg_2Si is approximately 1 μm in diameter and CMS is also spherical with the diameter of about 10 μm. In addition, the diameter of CNTs was about 50 nm and the length was larger than 500 nm. For Mg_2Si/CNTs materials, it could be observed that Mg_2Si surface was coated or surrounded by some CNTs as shown in Fig. 3d. However, Mg_2Si mainly coats on the surface of CMS in Mg_2Si/CMS composite materials. The differences in morphology and distribution of carbon materials in the composite materials may be caused by the difference of the size and shape of carbon materials. It will affect the electrochemical performance of the composite materials.

3.3. Electrochemical performance of the samples

The discharge capacity curves against the cycle number of the two composites are shown in Fig. 4. From these results, it is shown that the first discharge capacity of pure Mg_2Si was 580 mAh g^{-1}, but the capacity decreased to 50 mAh g^{-1} after 5 cycles. The pure Mg_2Si materials exhibit very poor cyclic stability. However, after formation of composite with CMS and CNTs, the electrochemical performance of the Mg_2Si are greatly improved, i.e. the electrochemical properties of all the composites are much better than pure Mg_2Si materials. For example, when the content of CNTs was 40%, the performance of the Mg_2Si is greatly improved as shown in Fig. 4a. The material delivers initial capacity of about 800 m mAh g^{-1} at the first cycle, and the capacity is kept at about 480 mAh g^{-1} after 5 cycles and still has a capacity of about 400 mAh g^{-1} after 30 cycles. As shown in Fig. 4b, the electrochemical properties of a series of Mg_2Si/CMS composite materials were also better than pure CMS, pure Mg_2Si and even Mg_2Si/CNTs materials with the same ratio. All discharge capacity of the composites such as CMS30, CMS40 and CMS50 at 5th cycle was held on about 500 mAh g^{-1}. Therefore, cyclic stability of the Mg_2Si materials has been improved greatly.

Fig. 5 shows the differential capacity plots (DCPs) in the first and tenth charge/discharge cycle between 0.02 and 3.0 V versus Li for CMS, Mg_2Si and CMS40 materials. As shown, in the first cathodic process, there are two weak peaks at 0.77 and 0.10 V for CMS material and three peaks at 0.15, 0.2 and 0.67 V for pure Mg_2Si material. However, for CMS40 composite material, there are a stronger peak at 0.73 V and a very sharp peak at 0.11 V. In the tenth cathodic process, the peaks at about 0.7 V

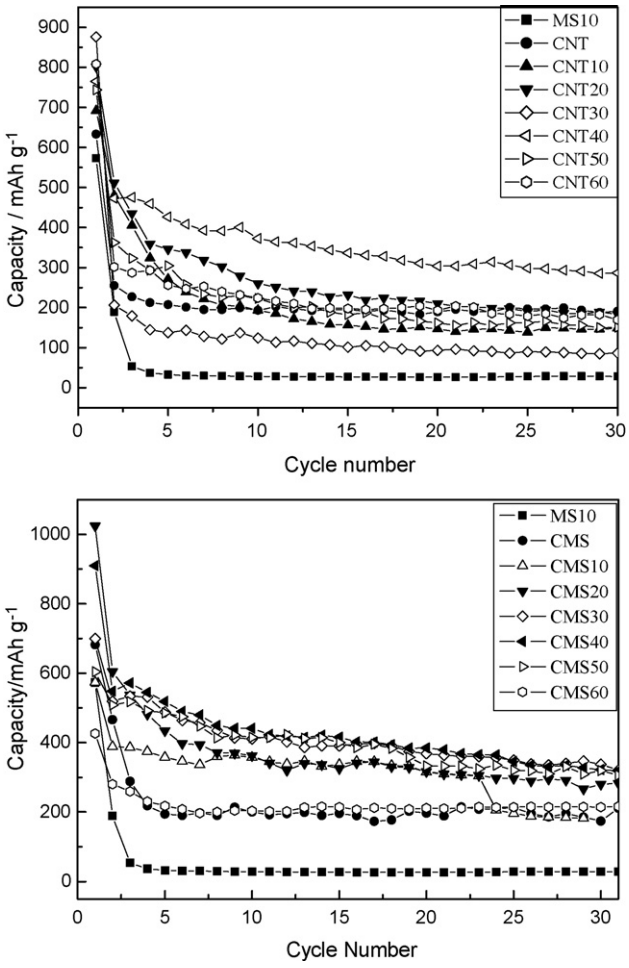

Fig. 4. The discharge capacity curves against the cycle number of the composite samples with 50 mA g^{-1} current at the range of 0.02–3.0 V. (a) Mg_2Si (MS10), carbon nanotubes (CNT) and Mg_2Si/CNTs composite with different carbon ratio; (b) Mg_2Si (MS10), CMS and Mg_2Si/CMS composite with different carbon ratio.

disappeared for all three materials. Therefore, the peak at 0.73 V of CMS40 material can be assigned to the formation of SEI layer. Comparing the peak intensity at lower potential (about 0.10 V) of these three materials, the peak intensity of CMS is weak, whereas the peak intensity of Mg_2Si and CMS40 is similar. Therefore, the peak at 0.11 V of CMS40 is mainly caused by lithium insertion into Mg_2Si. It is noted that there is only a single peak at 0.11 V in CMS40, whereas there are two peaks at 0.15 and 0.2 V in Mg_2Si. It indicated that there are some interaction between Mg_2Si and CMS, we think that this interaction is a kind of "constrained effects", i.e. the addition of CMS material in the composites offered a versatile matrix, it could be also thought as a kind of structure with "constrained effects" for Mg_2Si and depress the volume changes during the electrochemical processes, thus the cyclic stabilities of the composites are improved. In the first anodic process, there are three peaks at 0.21, 0.3 and 0.64 V for both of Mg_2Si and CMS40, whereas CMS has only a weak peak at about 0.15 V. However, there are not observable peak in the tenth cycle for pure Mg_2Si, which indicate that the capacity-fading rate of the pure Mg_2Si material is very fast. In contrast, the peaks of CMS40 have not almost change, and the peak at 0.64 V

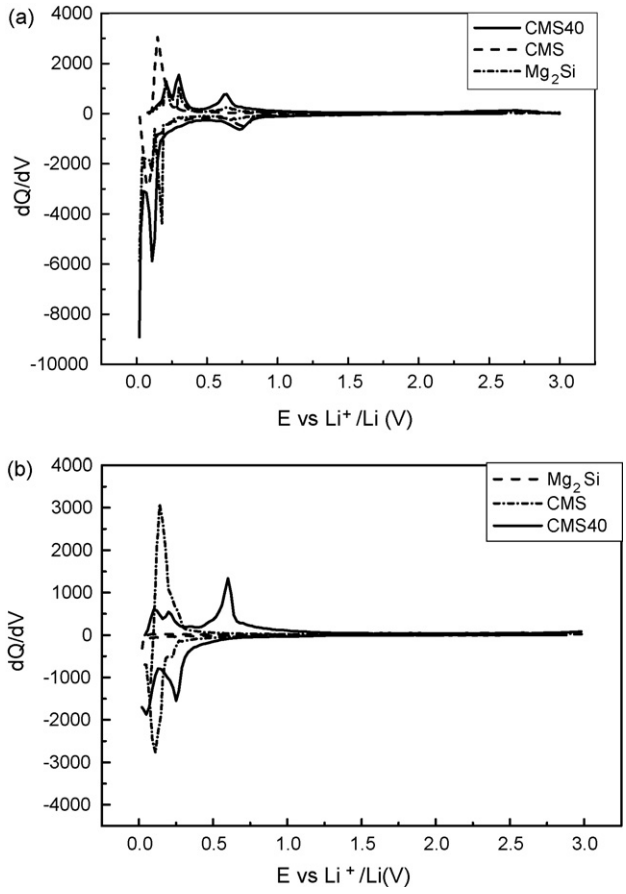

Fig. 5. DCPs for Mg_2Si, CMS and CMS40 composite materials cycled between 0.02 and 3.0 V vs. Li. in the first and tenth charge/discharge cycle. (a) In the first cycle; (b) in the tenth cycle. The magnified DCPs figure between 0.02 and 1.5 V shown in inset.

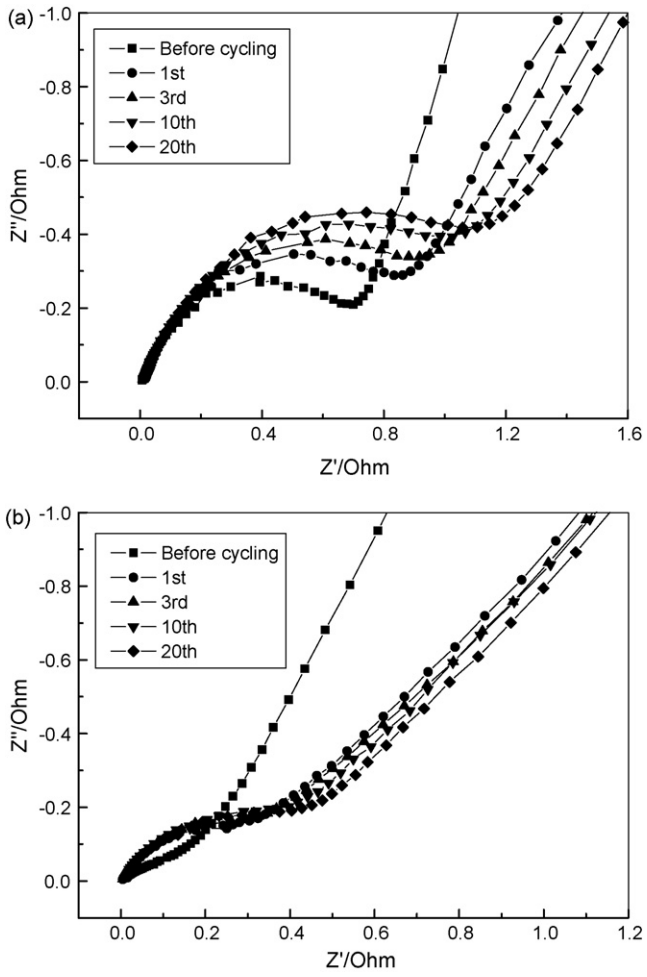

Fig. 6. The ac impedance spectra of three electrodes system with Mg_2Si (a) and Mg_2Si/CMS40 composites (b).

of the CMS40 composite material even become stronger, which may be caused by the interaction between Mg_2Si and CMS as defined as "constrained effects". For pure CMS material, the peaks have nearly no changes, indicating a good reversibility of the CMS materials.

In order to understand the intrinsic improving mechanism of cyclic performance of the composites, some preliminary electrochemical and spectroscopy experiments have been done. For example, EIS experiments of the pure Mg_2Si and CMS40 composite electrodes were carried out before cycling and after different cycle times. The ac impedance spectra of three electrodes system with Mg_2Si and CMS40 composites as working electrodes are illustrated in Fig. 6. All of the EIS spectra contain a high frequency semi-circle and a low frequency straight line. The semi-circle is mainly attributed to charge-transfer impedance of the electrode/electrolyte interface, thus some information of eletrode surface reaction can be obtained from the changes of semi-circle. It is clear from the figure that pronounced difference appears at the semi-circle. As shown in Fig. 6a, the diameters of semi-circle of Mg_2Si enlarged from 0.7 Ω before cycling to 1.2 Ω at 20th cycle, i.e. the charge impedence increased with cycles. By contrast, the diameters of semi-circle of CMS40 composite increase from 0.2 to 0.4 Ω after 1st cycle and have not obvious change in the following cycles. It indicates that CMS40 composite electrode not only has a lower charge-transfer resistance, but also has a quite stable reactive interface between electrode and electrolytes during the charge–discharge cycles, it correlates very well with previous charge–discharge experiments: the composite materials deliver higher discharge capacity and show much better cyclic stability.

4. Conclusions

In this paper, Mg_2Si/C composites are investigated as a possible anode material for rechargeable lithium ion batteries. It is demonstrated that a good Mg_2Si/C composites anode materials can be made by simply ball-milling of Mg_2Si and carbon materials such as CNTs or CMS. It is also shown that cyclic stability of the composite materials is strongly influenced by the content of carbon materials such as CNTs or CMS in the composites.

Under the optimized condition, the Mg_2Si/C composites can deliver a reversible capacity as high as 400 mAh g^{-1} with satisfied cyclic performance. The improving mechanism of the composite materials is also preliminarily studied. It is shown that composite electrode material has a lower charge-transfer resistance and a stable reactive interface based on EIS results. It is believed that the depression of the volume expansion con-

tributes the improvement of cyclic stability of the composite materials.

Acknowledgements

This work was supported by the National Natural Science Foundation of China (No.29925310, 20433060, 20473068).

References

[1] K.D. Kepler, J.T. Vaughey, M.M. Thackeray, Electrochem. Solid-State Lett. 2 (1999) 307.
[2] H. Li, L.H. Shi, W. Lu, X.J. Huang, L.Q. Chen, J. Electrochem. Soc. 148 (2001) A915.
[3] P. Poizot, S. Laruelle, S. Grugeon, L. Dupont, J.M. Tarascon, Nature 407 (2000) 496.
[4] S. Grugeon, S. Laruelle, R. Herrera-Urbina, L. Dupont, P. Poizot, J.M. Tarascon, J. Electrochem. Soc. 148 (2001) A285.
[5] D. Larcher, C. Masquelier, D. Bonnin, Y. Chabre, V. Masson, J.B. Leriche, J.M. Tarascon, J. Electrochem. Soc. 150 (2003) A133.
[6] F. Badway, I. Plitz, S. Grugeon, S. Laruelle, M. Dolle, A.S. Gozdz, J.M. Tarascon, Electrochem. Solid-State Lett. 5 (2002) A115.
[7] J. Yang, K. Wang, J.Y. Xie, J. Electrochem. Soc. 150 (2003) A140.
[8] T. Shodai, S. Okada, S. Tobishima, J. Yamaki, Solid State Ionics 86–88 (1996) 785.
[9] J.B. Kim, H.Y. Lee, K.S. Lee, S.H. Liu, S.M. Lee, Electrochem. Commun. 5 (2003) 544.
[10] S.W. Song, K.A. Striebel, X. Song, E.J. Cairns, J. Power Sources 119–121 (2003) 110.
[11] G.X. Wang, L. Sun, D.H. Bradhurst, S. Zhong, S.X. Dou, H.K. Liu, J. Alloys Compd. 306 (2000) 249.
[12] M. Wachtler, J.O. Besenhard, M. Winter, J. Power Source 94 (2001) 189.
[13] M. Wachtler, M. Winter, J.O. Besenhard, J. Power Source 105 (2002) 151.
[14] J. Wolfenstine, J. Power Sources 124 (2003) 241.
[15] Z. Shi, M. Liu, D. Naik, J. Gole, J. Power Sources 92 (2001) 70.
[16] W. Weydanz, M. Wohlfahrt-Mehrens, R. Huggins, J. Power Sources 81–82 (1999) 237.
[17] H. Kim, J. Choi, H. Sohn, T. Kang, J. Electrochem. Soc. 146 (1999) 4401.
[18] T. Moriga, K. Watanabe, D. Tsuji, S. Massaki, I. Nakabayashi, J. Solid State Chem. 153 (2000) 386.
[19] G.A. Roberts, E.J. Cairns, J.A. Reimer, J. Electrochem. Soc. 151 (2004) A493.
[20] J. Yang, B.F. Wang, K. Wang, Y. Liuand, J.Y. Xie, Z.S. Wen, Electrochem. Solid-State Lett. 6 (2003) A154.
[21] S. Kim, G.E. Blomgren, P.N. Kumta, Electrochem. Solid-State Lett. 7 (2004) A44–A48.
[22] X.Z. Liao, Z.F. Ma, H.H. Hu, Y.Z. Sun, X.X. Yuan, Electrochem. Commun. 5 (2003) 657.
[23] W.X. Chen, J.Y. Lee, Z.L. Liu, Carbon 41 (2003) 959.
[24] Z.S. Wen, J. Yang, B.F. Wang, K. Wang, Y. Liu, Electrochem. Commun. 5 (2003) 165.
[25] Y. Wang, J.Y. Lee, B.H. Chen, Electrochem. Solid-State Lett. 6 (2003) A19.
[26] H. Honda, H. Sakaguchi, I. Tanaka, T. Esaka, J. Power Sources 123 (2003) 216.
[27] B. Veeraraghavan, A. Durairajan, B. Haran, B. Popov, R. Guidotti, J. Electrochem. Soc. 149 (2002) A675.
[28] G.X. Wang, J.H. Ahn, M.J. Lindsay, L. Sun, D.H. Bradhurst, S.X. Dou, H.K. Liu, J. Power Sources 97-8 (2001) 211.
[29] Read, D. Foster, J. Wolfenstine, W. Behl, J. Power Sources 96 (2001) 277.
[30] H.Y. Lee, S.M. Lee, J. Power Sources 112 (2002) 649.
[31] G.A. Roberts, E.J. Cairns, J.A. Reimer, J. Power Sources 110 (2002) 424.
[32] P. Chen, H.B. Zhang, G.D. Lin, Q. Hong, K.R. Tsai, Carbon 35 (1997) 1495.
[33] J.M. Yan, H.Z. Huang, J. Zhang, Z.J. Liu, Y. Yang, J. Power Sources 146 (2005) 264.
[34] Z.R. Zhang, H.S. Liu, Z.L. Gong, Y. Yang, J. Power Sources 129 (1) (2004) 101.